

Characterization of Pineal Region in MR Brain Images using Texture Analysis

Mazin B. A. Hassib^{1,2}, Ahmed B. A. Hassib¹, Abbas K. A. Ibrahim³, Asma I. A. Alamin², M. E. M. Garelnabi^{1,2}

1 Faculty of Radiology and Medical Imaging Sciences - National University, Sudan-Khartoum

2 College of Medical Radiologic Sciences- Sudan University of Science and Technology, Sudan-Khartoum

3 College of Medical Radiological Science and Nuclear Medicine, AlRibat National University, Khartoum, Sudan

Corresponding Author: MazinHassib

Abstract: *The classification processes of MRI brain were defining the corpus, pineal gland, techunum, and third ventricle were carried out using Interactive Data Language (IDL) program as platform for the generated codes. The result of the classification showed that the pineal gland areas were classified well from the rest of the tissues although it has characteristics mostly similar to surrounding tissue.*

The results show that the Gray Level variation and features give classification accuracy

Several texture features are introduced using Gray Level variation and features and the FOS gives a classification score matrix generated by linear discriminate analysis and the overall classification accuracy was 92.7%, were the classification accuracy of corpus 93.3%, pineal gland 97.9%, techunum 89.9%, while the third ventricle showed classification accuracy 88.5%. These relationships are stored in a Texture Dictionary that can be later used to automatically annotate new MRI with the appropriate pineal gland

Key words: *corpus, pineal gland, third ventricle, texture analysis, FOS, MRI*

Date of Submission: 23-09-2018

Date of acceptance: 08-10-2018

I. Introduction

Signs and symptoms related to pineal lesions are generally secondary to mass effect on adjacent structures. Compression of the tectal plate can result in obstruction of the sylvian aqueduct and obstructive hydrocephalus. Cerebellar, corticospinal or sensory disturbance can result from direct

compression of the midbrain [1]. Infiltrative lesions of the pineal gland may interfere with normal pineal gland function and lead to precocious puberty, less commonly hypogonadism and diabetes insipidus. Pineal parenchymal lesions account for less than 15 % of all pineal masses and less than 0.2 % of intracranial neoplasms [1,2]. These lesions commonly arise from pineocytes or their precursors and are classified by the World Health Organization (WHO) into the following entities: low-grade pineocytoma, pineal parenchymal tumour of intermediate differentiation (PPTID), papillary tumour of pineal region (PTPR) and highly malignant pineoblastoma [3].

It was reported that several physiological or pathological conditions indeed alter the morphology of the pineal glands. For example, the pineal gland of obese individuals is usually significantly smaller than that in a lean subject [4]. The pineal volume is also significantly reduced in patients with primary insomnia compared to healthy controls and further studies are needed to clarify whether low pineal volume is the basis or a consequence of a functional sleep disorder [5]. These observations indicate that the phenotype of the pineal gland may be changeable by health status or by environmental factors, even in humans. The largest pineal gland was recorded in new born South Pole seals; it occupies one third of their entire brain [6,7]. The pineal size decreases as they grow. Even in the adult seal, however, the pineal gland is considerably large and its weight can reach up to approximately 4000 mg, 27 times larger than that of a human. This huge pineal gland is attributed to the harsh survival environments these animals experience [8].

Recent advances in MRI imaging have led to the development of novel gradient echo (GRE) imaging techniques such as SWMR, which is based on magnetic susceptibility and sensitive to materials distorting the local magnetic field. SWMR allows for a reliable differentiation of calcifications from tissue artifacts, hemorrhage and other causes of susceptibility differences by using T2_{*} Diagnostic accuracy of SWMR for the evaluation of pineal gland calcification weighted magnitude and GRE filtered-phase information to generate a unique contrast [9-13].

II. Material and methods

159 consecutive patients (male=93, Female 66) their ages were between (19-31) years who had undergone 3D-T1 Brain MRI Scan. Excluded Patients were those who had mid brain & endocrine diseases. Detailed Demographic Information of Population including; age,gender, weight,height, and BMI was recorded.

MRI machine Toshiba TM 1.5 T as used at Al-Mouleem Hospital, the sequence Were: Ultrafast Gradient Echo 3D with preparation Pulse T₁W(3D-FEE) SENSE + head Coil; Specific Absorption Rate =0.3199, Flip Angle 30 degree, ETL=1 Echo No.=1, Slice Thickness =1.6mm, Gap Between Slice = 50% .TR=0.8ms / TE = 2.6ms. Matrix 256 px X 256 px.

Statistical Methods

First Order Statistics: FOS can be used as the most basic texture feature extraction methods, which are based on the probability of pixel intensity values occurring in digital images. The parameters in the following statistical formulas are x_i , the intensity value of pixel i , N , the total number of pixels, $\max V$, the maximum intensity value within a patch and H_i , the histogram of an image patch.

Mean: Calculates the mean intensity value of all pixels. the function $\mu = \text{mean2(IP)}$ can be used to compute this feature.

$$\mu = \frac{1}{N} \sum_{i=1}^N x_i$$

Standard Deviation :

The standard deviation of all the intensity values of a patch is used as a texture feature. The corresponding Matlab function is $\sigma = \text{std2(IP)}$.

$$\sigma = \sqrt{\frac{1}{N} \sum_{i=1}^N (x_i - \mu)^2}$$

Coefficient of variation

The coefficient of variation can be seen as the relative standard deviation. It is calculated by dividing the standard deviation with the mean value.

$$c_v = \frac{\sigma}{\mu}$$

Entropy

The entropy of a gray-scale image is a measure of intensity value randomness. It is calculated from the histogram counts of an image giving a probability p of certain pixel values occurring in the image.

$$s = - \sum (p_i * \log_2(p_i))$$

Skewness

Another statistical measure which is used for texture analysis is skewness. It measures the symmetry of a distribution curve of pixel intensity occurrences as seen in a histogram. The function $\gamma_1 = \text{skewness(IP)}$ can be used to compute the skewness.

$$\gamma_1 = \frac{\frac{1}{N} \sum_{i=1}^N (x_i - \mu)^3}{\left(\frac{1}{N} \sum_{i=1}^N (x_i - \mu)^2\right)^{\frac{3}{2}}}$$

Kurtosis

The kurtosis measures the atness of a histogram relative to a normal distribution. A curve has a high kurtosis when it has a clear peak close to the mean value. The Matlab function for the kurtosis is $\gamma_2 = \text{kurtosis(IP)}$.

$$\gamma_2 = \frac{\frac{1}{N} \sum_{i=1}^N (x_i - \mu)^4}{\left(\frac{1}{N} \sum_{i=1}^N (x_i - \mu)^2\right)^2} - 3$$

III. Results and discussion

In this paper were features extracted from *MRI* using First order statistic and All these features were calculated for all images and then the data were ready for discrimination which was performed using step-wise technique in order to select the most significant feature that can be used to classify the MR brain imaging for Pineal Gland and the results show that:

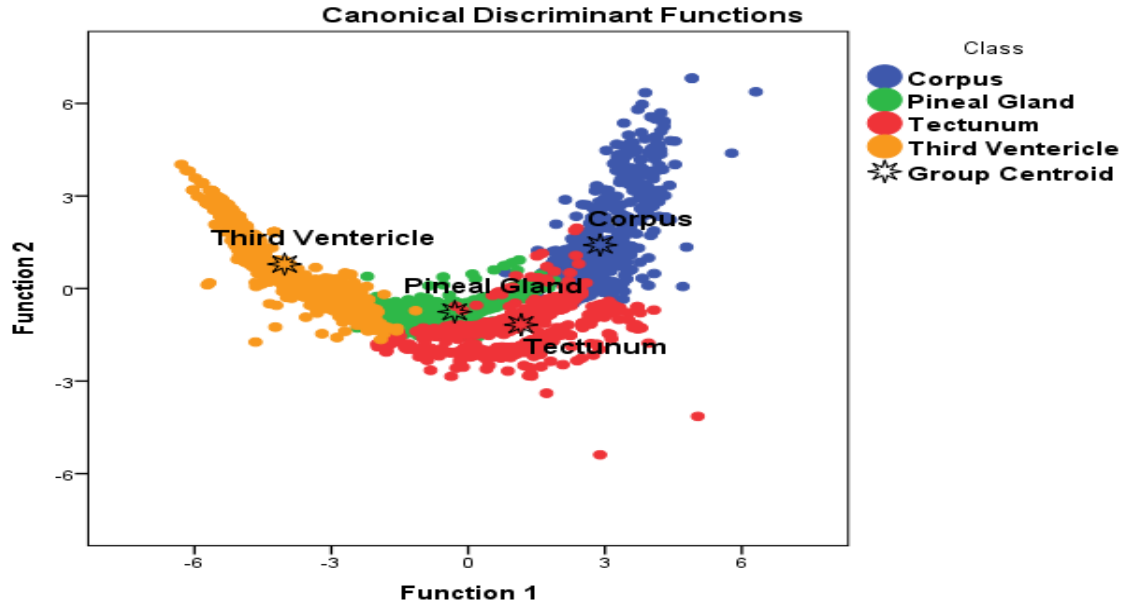


Fig 1. classification Map that created using linear discriminant analysis function.

Fig. 1. Scatter plot generated using discriminate analysis function for Four classes represents: Corpus, pineal gland, techunum, third ventricle the classification showed that the pineal gland were reclassified well from the rest of the tissues although it has characteristics mostly similar to surrounding tissue.

Table 1: Showed the classification accuracy of the Pineal Gland using linear discriminant analysis:

| Classes | | Predicted Group Membership | | | | Total |
|----------|-----------------|----------------------------|--------------|----------|-----------------|-------|
| | | Corpus | Pineal Gland | Tectunum | Third Ventricle | |
| Original | Corpus | 93.3 | 2.8 | 4.0 | .0 | 100.0 |
| | Pineal Gland | .8 | 97.9 | 1.3 | .0 | 100.0 |
| | Tectunum | 1.9 | 8.3 | 89.9 | .0 | 100.0 |
| | Third Ventricle | .0 | 10.7 | .8 | 88.5 | 100.0 |

92.7% of original grouped cases correctly classified.

Table (1) show classification score matrix generated by linear discriminate analysis and the overall classification accuracy of corpus 93.3%, were the classification accuracy of pineal gland 97.9%, techunum 89.9%, While the third ventricle showed a classification accuracy 88.5%.

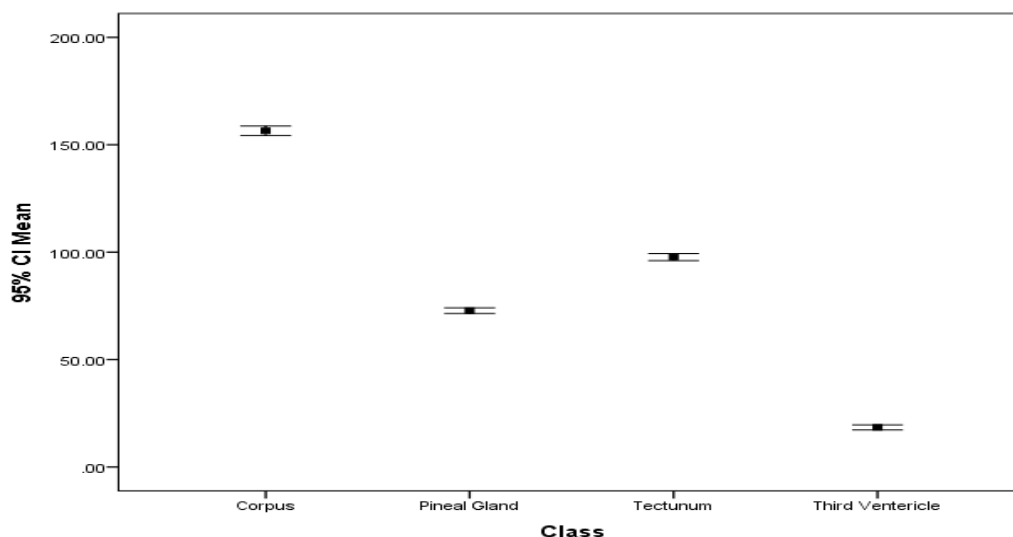


Fig .1 show error bar plot for the CI meantexturalfeatures that selected by the linear stepwise discriminatefunction as a discriminate feature where it discriminates between all features. From the discriminate power point of view in respect tothe applied features the mean candifferentiate between all the classes successfully.

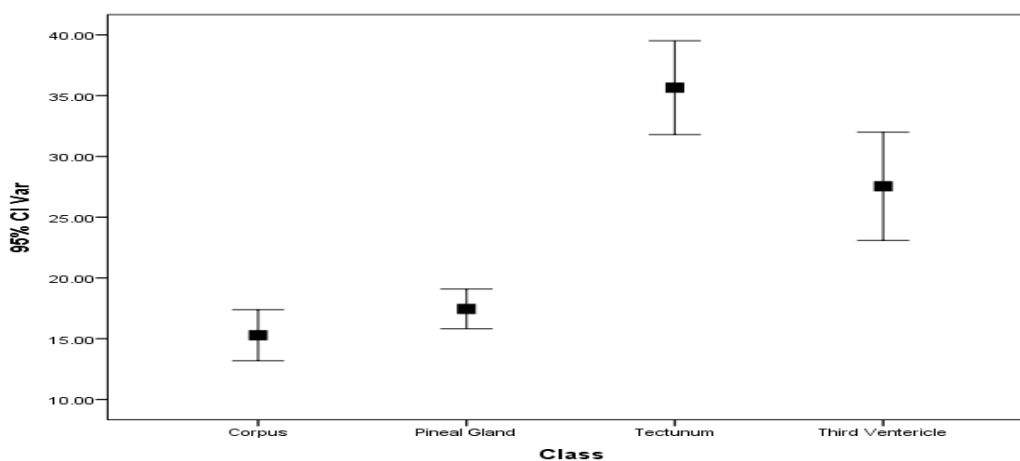


Fig .2 show error bar plot for the variance textural features that selected by the linear stepwise discriminate function as a discriminate feature where it discriminates between all features.

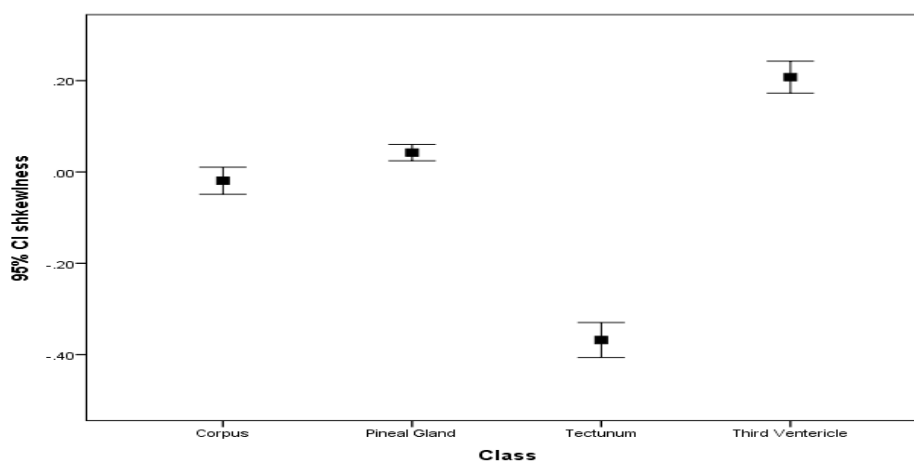


Fig .3 show error bar plot for the shkewness textural features that selected by the linear stepwise discriminate function as a discriminate feature where it discriminates between all features.

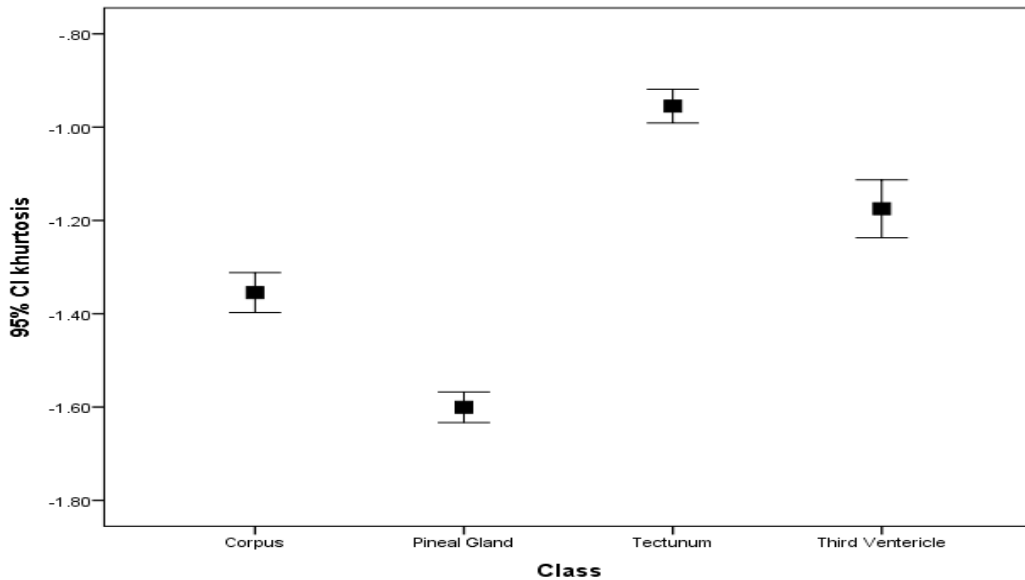


Fig .4 show error bar plot for the kurtosis texture features that selected by the linear stepwise discriminate function as a discriminate feature where it discriminates between all features.

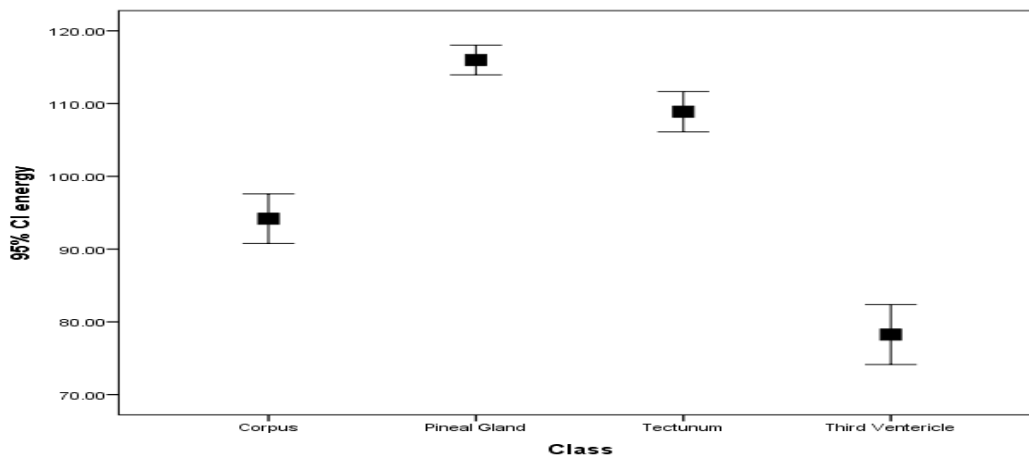


Fig .5 show error bar plot for the energy texture features that selected by the linear stepwise discriminate function as a discriminate feature where it discriminates between all features.

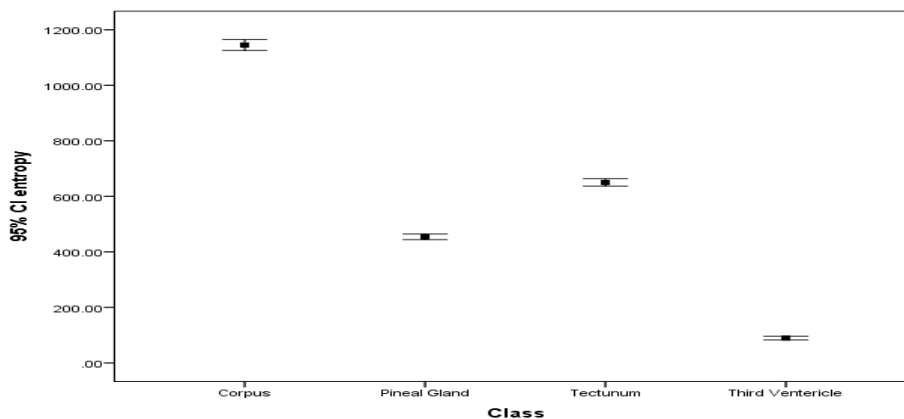


Fig .6 show error bar plot for the CI entropy textural features that selected by the linear stepwise discriminate function as a discriminate feature where it discriminates between all features. From the discriminate power point of view in respect to the applied features the entropy can differentiate between all the classes successfully.

IV. Conclusion

The classification processes of *MRI* brain were defining the corpus, pineal gland, tectum, and third ventricle were carried out using Interactive Data Language (IDL) program as platform for the generated codes. The result of the classification showed that the pineal gland areas were classified well from the rest of the tissues although it has **characteristics mostly similar to surrounding tissue**.

Several texture features are introduced from FOS and the classification score matrix generated by linear discriminate analysis and the overall classification accuracy was 92.7%, were the classification accuracy of corpus 93.3%, pineal gland 97.9%, tectum 89.9%, While the third ventricle showed a classification accuracy 88.5%.

Using Linear discrimination analysis generated a classification function which can be used to classify other image into the mentioned classes as using the following multi-regression equation;

$$\text{Corpus} = (\text{Mean} + 2.233) * \text{variance} + (-0.046) * (\text{Skewness} + 1.398) * (\text{kurtosis} + 0.203) * (\text{energy} + (-0.013)) * \text{entropy} + (-0.239) - 38.185$$

$$\text{Pineal Gland} = (\text{Mean} + 2.123) * \text{variance} + (-0.033) * (\text{Skewness} + 1.584) * (\text{kurtosis} + (-0.977)) * (\text{energy} + 0.011) * \text{entropy} + (-0.247) - 23.713$$

$$\text{Tectum} = (\text{Mean} + 2.453) * \text{variance} + (-0.023) * (\text{Skewness} + (-1.520)) * (\text{kurtosis} + 2.021) * (\text{energy} + 0.001) * \text{entropy} + (-0.281) - 28.785$$

$$\text{Third Ventricle} = (\text{Mean} + 0.687) * \text{variance} + (-0.003) * (\text{Skewness} + 2.124) * (\text{kurtosis} + (-2.148)) * (\text{energy} + 0.023) * \text{entropy} + (-0.083) - 6.36$$

References

- [1]. Klein P, Rubinstein LJ (1989) Benign symptomatic glial cysts of the pineal gland: a report of seven cases and review of the literature. *J Neurol Neurosurg Psychiatry* 52:991–995
- [2]. Surawicz TS, McCarthy BJ, Kupelian V et al (1999) Descriptive epidemiology of primary brain and CNS tumors: results from the Central Brain Tumor Registry of the United States, 1990-1994. *NeuroOncol* 1(1):14–25
- [3]. Louis DN, Ohgaki H, Wiestler OD, Cavenee WK (2007) WHO classification of tumors of the central nervous system. IARC Press, Lyon.
- [4]. Grosshans, M.; Vollmert, C.; Vollstaedt-Klein, S.; Nolte, I.; Schwarz, E.; Wagner, X.; Leweke, M.; Mutschler, J.; Kiefer, F.; Bumb, J.M. The association of pineal gland volume and body mass in obese and normal weight individuals: A pilot study. *Psychiatr. Danub.* 2016, 28, 220–224. [PubMed]
- [5]. Bumb, J.M.; Schilling, C.; Enning, F.; Haddad, L.; Paul, F.; Lederbogen, F.; Deuschle, M.; Schredl, M.; Nolte, I. Pineal gland volume in primary insomnia and healthy controls: A magnetic resonance imaging study. *J. Sleep Res.* 2014, 23, 276–282. [CrossRef] [PubMed]
- [6]. Bryden, M.M.; Griffiths, D.J.; Kennaway, D.J.; Ledingham, J. The pineal gland is very large and active in newborn antarctic seals. *Experientia* 1986, 42, 564–566. [CrossRef] [PubMed]
- [7]. Cuello, A.C.; Tramezzani, J.H. The epiphysis cerebri of the Weddell seal: Its remarkable size and glandular pattern. *Gen. Comp. Endocrinol.* 1969, 12, 154–164. [CrossRef]
- [8]. Tan, D.X.; Manchester, L.C.; Sainz, R.M.; Mayo, J.C.; León, J.; Reiter, R.J. Physiological ischemia/reperfusion phenomena and their relation to endogenous melatonin production: A hypothesis. *Endocrine* 2005, 27, 149–158. [CrossRef]
- [9]. Haacke EM, Mittal S, Wu Z, Neelavalli J, Cheng YC. Susceptibility-weighted imaging: technical aspects and clinical applications, part 1. *AJNR Am J Neuroradiol.* 2009; 30(1):19–30. PubMed Central PMCID: PMC3805391. doi: 10.3174/ajnr.A1400 PMID: 19039041
- [10]. Mittal S, Wu Z, Neelavalli J, Haacke EM. Susceptibility-weighted imaging: technical aspects and clinical applications, part 2. *AJNR Am J Neuroradiol.* 2009; 30(2):232–52. PubMed Central PMCID: PMC3805373. doi: 10.3174/ajnr.A1461 PMID: 19131406
- [11]. Chen W, Zhu W, Kovanlikaya I, Kovanlikaya A, Liu T, Wang S, et al. Intracranial calcifications and hemorrhages: characterization with quantitative susceptibility mapping. *Radiology.* 2014; 270(2):496–505. PubMed Central PMCID: PMC4228745. doi: 10.1148/radiol.13122640 PMID: 24126366
- [12]. Buch S, Cheng YN, Hu J, Liu S, Beaver J, Rajagovindan R, et al. Determination of detection sensitivity for cerebral microbleeds using susceptibility-weighted imaging. *NMR in biomedicine.* 2016.
- [13]. Nandigam RN, Viswanathan A, Delgado P, Skehan ME, Smith EE, Rosand J, et al. MR imaging detection of cerebral microbleeds: effect of susceptibility-weighted imaging, section thickness, and field strength. *AJNR American journal of neuroradiology.* 2009; 30(2):338–43. PubMed Central PMCID: PMC2760298. doi: 10.3174/ajnr.A1355 PMID: 19001544

Mazin Hassib. "Characterization of Pineal Region in MR Brain Images using Texture Analysis." *IOSR Journal of Applied Physics (IOSR-JAP)*, vol. 10, no. 5, 2018, pp. 32-37.